

University of Arkansas, Fayetteville

ScholarWorks@UARK

Chemical Engineering Faculty Publications and Presentations

Chemical Engineering

4-23-2021

Peptoid Microsphere Coatings to Improve Performance in Sandwich ELISA Microarrays

Jesse L. Roberts

University of Arkansas, Fayetteville

German R. Perez Bakovic

University of Arkansas, Fayetteville

Shannon L. Servoss

University of Arkansas, Fayetteville, sservoss@uark.edu

Follow this and additional works at: <https://scholarworks.uark.edu/chegpub>



Part of the [Microarrays Commons](#), [Polymer Science Commons](#), and the [Process Control and Systems Commons](#)

Citation

Roberts, J. L., Perez Bakovic, G. R., & Servoss, S. L. (2021). Peptoid Microsphere Coatings to Improve Performance in Sandwich ELISA Microarrays. *Sensing and Bio-Sensing Research*, 32, 100424. <https://doi.org/10.1016/j.sbsr.2021.100424>

This Article is brought to you for free and open access by the Chemical Engineering at ScholarWorks@UARK. It has been accepted for inclusion in Chemical Engineering Faculty Publications and Presentations by an authorized administrator of ScholarWorks@UARK. For more information, please contact scholar@uark.edu, uarepos@uark.edu.



Peptoid microsphere coatings to improve performance in sandwich ELISA microarrays

Jesse L. Roberts, German R. Perez Bakovic, Shannon L. Servoss*

University of Arkansas, Ralph E. Martin Department of Chemical Engineering, 3202 Bell Engineering Center, 1 University of Arkansas, Fayetteville, AR 72701, United States of America

ARTICLE INFO

Keywords:
Peptoid
ELISA
Microarray
Microspheres

ABSTRACT

Enzyme-linked immunosorbent assay (ELISA) microarray performance is limited by low assay sensitivity and dynamic range. Increasing the surface area for reagent binding can help to improve performance, but standard techniques such as roughening the surface or adding a polymer coating lead to increased non-specific fluorescence and do not have reproducibly improved performance. Another approach to increase surface area is adding a microsphere coating on the surface. Poly-N-substituted glycine (peptoid) microspheres are ideal for this application due to low immunogenicity, protease-resistance, and biocompatibility. Peptoids are polymers with a backbone similar to peptides, but with the side chains appended to nitrogen rather than the alpha carbon. A variety of side chain chemistries can be incorporated into peptoids through a solid-phase, sequence-specific synthesis protocol. Here we report the development of sandwich ELISA microarray on peptoid microsphere coated glass slides. Coating morphology was evaluated via SEM and efficacy was assessed by ELISA microarray performance. Peptoid microsphere coated glass slides exhibit an increase in signal intensity and dynamic range as compared to commercially available microarray slides. These studies show the potential for peptoid microspheres as coatings for ELISA microarray slides, as well as for use in other biosensor applications.

1. Introduction

Over the last several decades there have been numerous publications focused on the development of sensitive, disease-specific assays to assist in therapeutic decisions [1–5]. Early disease detection decreases economic costs, improves treatment options, and reduces mortality [6]. Biomarker-based technologies, including enzyme-linked immunosorbent assay (ELISA) microarray and bead-based immunoassay, offer platforms for sensitive and specific disease detection [7]. Multiplex bead array assays (MBAA) such as Luminex, xMap [8], Smartbead UltraPlex [9], and flow cytometry technologies [10] offer promising, high-throughput methods of detecting cytokines and other analytes in serum and plasma samples. MBAA make it possible to perform immunoassays in a multiplexed design to independently and qualitatively analyze multiple samples at one time. For instance, the xMAP technique utilizes hundreds of uniquely colored beads, ranging from much larger magnetic beads (6.5 μm) to smaller non-magnetic beads ($\sim 1 \mu\text{m}$),

created by two different fluorescent dyes to simultaneously identify multiple analytes [8]. However, a key concern in the viability of MBAA is the potential for interference between analyte samples. The antibodies on each bead may cross-react with other antibodies, cross-species antibodies, and molecules, ultimately reducing the efficacy of the MBAA techniques and requiring additional testing to ensure no cross-reacting has occurred [11].

ELISA microarray technology has emerged as a strong platform for the analysis of biomarkers due to its ability to quantify low-abundance proteins in complex biological fluids over large concentration ranges [12,2]. ELISA microarray eliminates the cross-reactivity that is commonly seen in MBAA by focusing on a single analyte at a time. The use of matched high-affinity antibody pairs to target a single antigen results in unmatched sensitivity and specificity. The miniature scale of the platform allows for cost-effective and efficient parallel screening of small sample volumes in a high-throughput manner [12]. The slide chemistry and morphology is crucial for optimal performance of ELISA

Abbreviations: ELISA, enzyme-linked immunosorbent assay; DSS, Disuccinimidyl suberate; BS³, bis[sulfosuccinimidyl] suberate; PBS, phosphate-buffered saline; TSA, Tyramide Signal Amplification; DMF, dimethylformamide; TFA, trifluoroacetic acid; HPLC, high-performance liquid chromatography; MALDI-TOF, matrix assisted laser desorption/ionization time of flight mass spectrometry; SEM, scanning electron microscope; PBS-T, PBS containing 0.05% Tween-20.

* Corresponding author.

E-mail address: sservoss@uark.edu (S.L. Servoss).

<https://doi.org/10.1016/j.sbsr.2021.100424>

Received 3 February 2021; Received in revised form 9 April 2021; Accepted 19 April 2021

Available online 23 April 2021

2214-1804/© 2021 The Author(s).

Published by Elsevier B.V. This is an open access article under the CC BY-NC-ND license

(<http://creativecommons.org/licenses/by-nc-nd/4.0/>).

microarray, as is evident by the large number of slide chemistries commercially available [13–18,4]. The slides must allow antibodies to be immobilized in a manner that maintains protein binding affinity while retaining high binding capacities, high signal-to-noise ratios, and high reproducibility [19]. Additionally, the high-throughput nature of the platform requires substrates to be robust and retain high levels of specificity and sensitivity through rigorous processing conditions and prolonged storage periods. While poly-L-lysine slides have emerged as promising slide chemistry due to strong antibody attachment via adsorption and high signal-to-noise ratio [20,21], ELISA microarray performance can be further improved by increasing the surface area for antibody attachment. In theory, increasing the surface area for antibody attachment should enhance the microarray results by providing more sites of attachment to increase signal intensity and the dynamic range. Polymer-based surfaces that increase surface area such as polyacrylamide [5,22], agarose [23], and nitrocellulose [24–28] suffer from low signal-to-noise ratios due to absorption of protein in the porous coating [20,21].

Poly-N-substituted glycines (peptoids) are promising as coatings for microarray slides due to their low immunogenicity, ease of synthesis, variety of available side chain chemistries, and the ability to form supramolecular structures that can increase surface area [29]. Peptoids are bioinspired, peptidomimetic polymers with a backbone structure closely resembling that of peptides, but with the side chains appended to the amide groups rather than the alpha-carbons. This structural modification prevents proteolytic degradation, making peptoids attractive as biocompatible materials. However, this modification also removes the presence of backbone amide hydrogens, which are critical for the formation of the hydrogen bond linkages that stabilize beta sheets and helices in peptides. Introduction of steric hindrance through side chain chemistry allows for the formation of secondary structures including turns [30,31], loops [32], and helices [33–37], as well as supramolecular assemblies such as superhelices [38], nanosheets [39], nanotubes [40], and microspheres [41].

Our lab has previously shown that partially water-soluble, helical peptoids self-assemble into microspheres [37] and can form uniform surface coatings [44]. The peptoid sequence, referred to as P3 (Fig. 1), includes chiral, aromatic side chains on two faces of the helix to induce the formation of helical secondary structure [41]. The third face of the helix, which offers considerable flexibility of design, contains methoxy and amine groups to increase water solubility. The amine groups enable covalent linkage to and electrostatic interactions with the slide surface. The secondary structure of P3 was determined by circular dichroism, which confirms polyproline type-I-like secondary structure [35].

In this study, we report the development of peptoid microsphere coated glass substrates for use in sandwich ELISA microarray. The morphology and uniformity of the coatings was evaluated by SEM and the coating efficacy was analyzed by ELISA microarray with known antibody pairs. The peptoid microsphere coated surfaces were found to exhibit higher signal intensity and dynamic range as compared to commercially available microarray slides.

2. Materials and methods

2.1. Materials

4-methoxybenzylamine and (*S*)-methylbenzylamine were purchased from Acros Organics (Pittsburgh, PA). *tert*-butyl N-(4-aminobutyl) carbamate was purchased from CNH Technologies Inc. (Woburn, MA). MBHA rink amide resin was purchased from NovaBiochem (Gibbstown, NJ). Piperidine was purchased from Sigma-Aldrich (St. Louis, MO). Test grade silicon wafers were purchased from University Wafer (South Boston, MA). Poly-L-lysine and ultra clean glass microarray slides were purchased from Thermo Scientific (Pittsburgh, PA). Disuccinimidyl suberate (DSS) and bis[sulfosuccinimidyl] suberate (BS³) were purchased from Pierce (Rockford, IL, USA). Purified antibodies and antigens were purchased from R&D Systems (Minneapolis, MN, USA). Blocking solution containing 10 mg/ml casein in phosphate-buffered saline, pH 7.2 (PBS) was purchased from Bio Rad Laboratories (Hercules, CA, USA). Tyramide Signal Amplification (TSA) system, including streptavidin-conjugated horseradish peroxidase, amplification diluent, and biotinyl tyramide, was purchased from Perkin Elmer (Wellesley, MA, USA). Alexa647-conjugated streptavidin was purchased from Invitrogen Life Technologies (Gaithersburg, MD). All other reagents were purchased from VWR (Radnor, PA). Chemicals were used without further modifications unless otherwise specified.

2.2. Peptoid synthesis

Peptoids were synthesized via the submonomer solid-phase method on rink amide resin, as previously described [42]. Briefly, the resin was swelled with dimethylformamide (DMF) and the Fmoc protecting group was removed using a 20% solution of piperidine in DMF. The resin-bound secondary amine was acylated with 0.4 M bromoacetic acid in DMF in the presence of *N,N'*-diisopropyl carbodiimide. Amine submonomers were incorporated via an S_N2 nucleophilic substitution reaction with primary amine in DMF. The two-step bromoacetylation and nucleophilic substitution cycle was repeated until all desired side chains were incorporated. The peptoid was cleaved from the resin using a mixture of 95% trifluoroacetic acid (TFA), 2.5% water, and 2.5% triisopropylsilane, and the acid was removed using a Heidolph Laborota 4001 rotary evaporator (Elk Grove Village, IL). The peptoid was lyophilized to a powder using a Labconco lyophilizer (Kansas City, MO) and diluted to a concentration of ~3 mg/ml in a 50:50 acetonitrile-water solution.

2.3. Peptoid purification

Peptoids were purified using a Waters Delta 600 preparative high-performance liquid chromatography (HPLC) instrument (Milford, MA) with a Duragel G C18 150 × 20 mm column (Peeke Scientific, Novato, CA) and a linear gradient of 35–95% solvent B (acetonitrile, 5% water, 0.1% TFA) in A (water, 5% acetonitrile, 0.1% TFA) over 60 min.

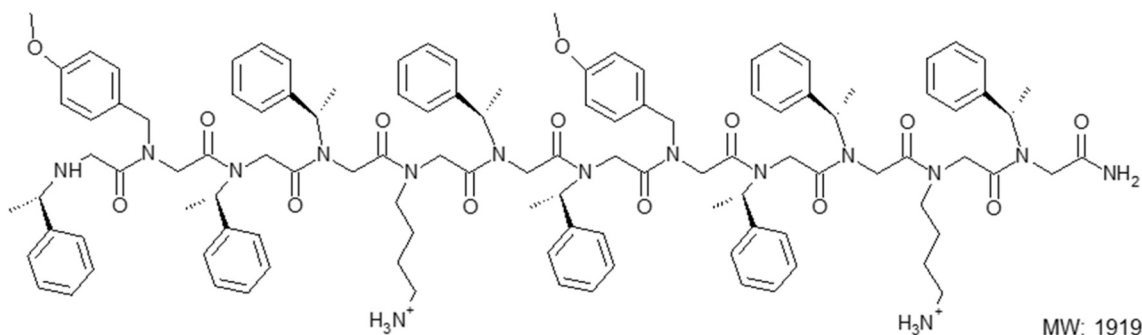


Fig. 1. Peptoid structure for the P3 sequence.

Peptoids were confirmed to be >98% pure via analytical HPLC (Waters Alliance, Milford, MA) with a Duragel G C18 150 × 2.1 mm column (Peeke Scientific) using a linear gradient of 35 to 95% solvent D (acetonitrile, 0.1% TFA) in C (water, 0.1% TFA) over 30 min. Purified peptoid fractions were lyophilized and stored as a powder at −20 °C.

2.4. Peptoid characterization

Synthesis of the desired peptoid sequence was confirmed via matrix assisted laser desorption/ionization time of flight mass spectrometry (MALDI-TOF; Bruker, Billerica, MA). Secondary structure was confirmed via CD spectrometry using a Jasco J-715 instrument (Easton, MD) at room temperature with a scanning speed of 20 nm/min and a path length of 0.1 mm. The peptoid was dissolved in methanol at a concentration of 120 μM. Each spectrum was the average of twenty accumulations.

2.5. Peptoid microsphere coatings

Peptoid microspheres were prepared by dissolving the peptoid in a 4:1 (v/v) ethanol/water solution at a concentration of 5 mg/ml, as previously described [41]. Glass slides (Erie Scientific, Portsmouth, NH) were outlined with an 8 × 2 array pattern using a Barnstead Thermolyne microarray slide imprinter (Dubuque, IA) to create a hydrophobic barrier for processing 16 wells per slide. The peptoid solution was applied to the glass surfaces and allowed to dry at room temperature and 60% relative humidity. Coating morphologies were visually assessed using a Phillips XL-30 scanning electron microscope (SEM; FEI, Hillsboro, OR).

2.6. Microsphere surface density distribution

Microsphere surface density distribution of the microsphere coatings was calculated using ImageJ software (National Institute of Health, MD). Noise reduction was completed with a fast Fourier transform (FFT) band-pass filter normalization, eliminating low- and high-spatial frequencies and transforming the original SEM images to a two-dimensional representation of the frequency. The images were converted to 8-bit grayscale and binarized adjusting the white and black threshold to optimize particle contrast with the background. Particle analysis was completed on the adjusted images to give an area percentage for the microsphere particles.

2.7. Microarray printing

ELISA microarray printing was performed at room temperature and 60% relative humidity as previously described [20]. Briefly, a GeSiM NanoPlotter 2.1 non-contact microarray printer with humidity control (Quantum Analytics, Foster City, CA, USA) was used to spot the antibodies. Prior to spotting, the microsphere coated surfaces, and in some cases the poly-L-lysine slides, were treated with a 0.3 mg/ml solution of the homo-bifunctional cross-linker BS³ in PBS for 20 min to create a reactive site for covalent attachment of antibodies via the amine groups. After incubation, the slides were rinsed in nanopure water and dried in a centrifuge. Capture antibodies were suspended in PBS to a concentration of 0.8 mg/ml and ~ 400 picoliters per spot were printed 500 μm apart in quintuplicate on each array. Upon completion, the antibodies were allowed to dry for an additional hour at 60% relative humidity. The slides were blocked with 10 mg/ml casein in PBS and processed immediately.

2.8. ELISA microarray

ELISA microarray was performed as previously described [20]. Briefly, all incubation steps were performed at room temperature in a closed, dark, humid chamber, with gentle mixing on an orbital shaker (Belly Dancer, Stovall Life Science, Greensboro, NC). A two-step wash

procedure between processing steps was performed by submerging the slides twice into PBS containing 0.05% Tween-20 (PBS-T). The slides were incubated with a mixture of antigen standards in 1 mg/ml casein in PBS overnight. Standard curves were created using a three-fold dilution series of the antigen mix along with an antigen-free blank for twelve total dilutions. Following a wash cycle, the slides were incubated with biotinylated detection antibody at 25 ng/ml in 1 mg/ml casein in PBS. The biotin signal was amplified using the TSA system following manufacturer instructions, and incubated with 1 μg/ml Alexa647-conjugated streptavidin in PBS-T. The slides were rinsed twice in PBS-T followed by deionized water.

A GenePix Autoloader 4200AL laser scanner (Molecular Devices, CA) was used to image the Alexa 647 fluorescence signal. The spot fluorescence intensity from the scanned slide images was quantified using GenePix Pro 3.0 software. Standard curves were created using ProMAT, a software program specifically developed for the analysis of ELISA microarray data based on a four-parameter logistic curves model [43]. The values for the lower limits of detection are calculated as the median concentration of the antigen-free blank plus three standard deviations [45]. In order to provide a value that is representative of all assays for comparisons, a relative limit of detection value was calculated using the median value for all assay replicates on each surface, as previously described [20]. Unless noted otherwise, results shown encompass three replicate experiments performed using slides that were coated, printed, and processed on independent occasions.

3. Results and discussion

3.1. Coating characterization

The formation of uniform peptoid microsphere coatings is essential to reduce variability in ELISA microarray. Coating morphology is directly linked to evaporation rate, requiring careful monitoring of drying conditions to ensure uniform sphere distribution and reproducible coatings. One issue observed in the formation of peptoid coatings is perimetral intensive deposition, often referred to as the “coffee ring effect,” in which denser coverage is observed at the perimeter of the coatings as compared to the center. Previous studies have shown that this effect is reduced when samples are evaporated at a constant contact area, which can be achieved by including surfactant in the microsphere solution [46]. The addition of Tween-20 to the peptoid microsphere solution results in improved coating uniformity, lessening perimetral microsphere deposition and allowing for an even distribution of microspheres on the surface (Fig. 2). At concentrations >0.1%, Tween-20 disrupts microspheres formation and alters microsphere size distribution (Fig. S1 in Supplemental Information). Previous work in our lab has focused on the reproducibility of the coatings, the physical properties of the microspheres, and their ability to withstand various conditions (pH, ionic strength, solvents) [36,47]. Using ImageJ particle analysis of SEM images, the average local microsphere surface density ($n = 10$) on the glass slides was 87% ($s = 2.59\%$) covered (Fig. S2 in Supplemental Information).

When antibodies were spotted directly on the peptoid microsphere coated slides, faint fluorescent signals were observed indicating weak adsorption of the antibodies to the surface. The homobifunctional linker, BS³, was used to covalently attach the antibodies to the peptoid microsphere coated slides (Fig. 3A). ELISA microarray results were reproducible for the slides with covalently attached antibodies. It should be noted that antibodies were not covalently attached to the poly-L-lysine surfaces because both our results (Fig. 3B) and findings by others [20] show no significant difference in ELISA microarray performance between adsorbed and covalently attached antibodies.

3.2. Coating efficacy for ELISA microarray

The efficacy of the peptoid microsphere coatings was evaluated by

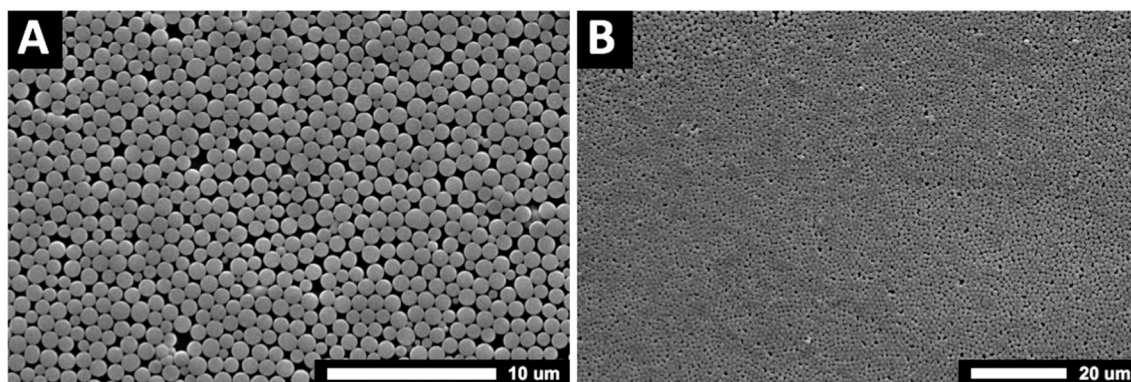


Fig. 2. Peptoid microsphere coated glass surfaces at (A) 3500× and (B) 1000× magnifications. Peptoids were dissolved in a 4:1 (v/v) ethanol/water solution at a concentration of 5 mg/ml. The peptoid solution was applied to the glass surfaces and allowed to dry at room temperature and 60% relative humidity.

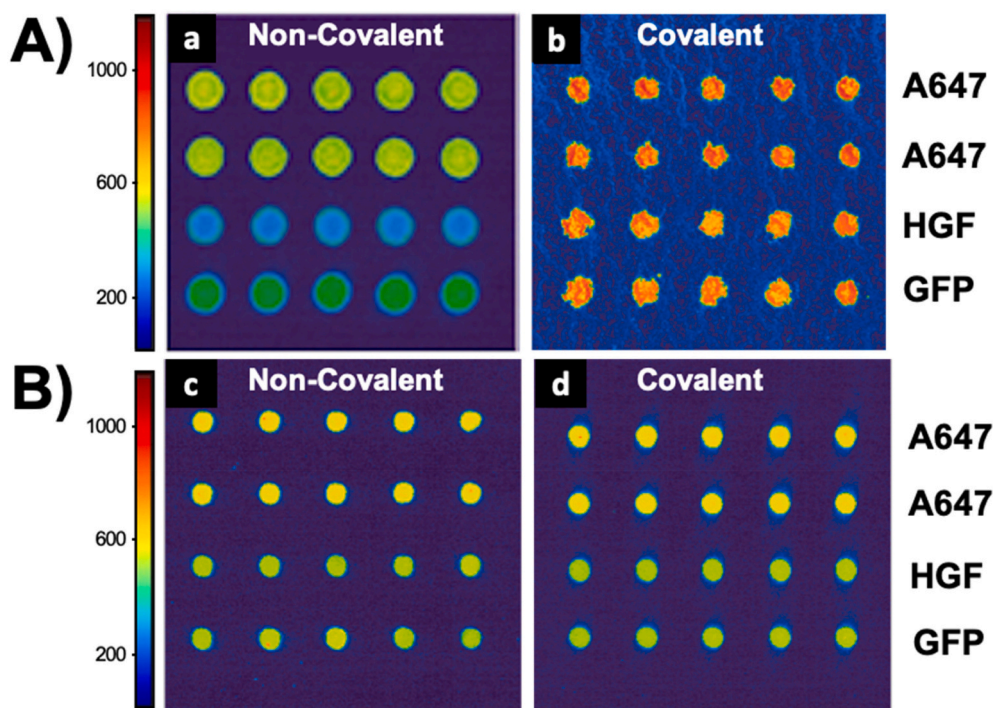


Fig. 3. (A) Images of fluorescence for GFP and HGF on peptoid microsphere coated glass surfaces with (a) non-covalent treated and (b) BS³ treated covalent surfaces. (B) Images of fluorescence for GFP and HGF on uncoated poly-L-lysine slides with (a) non-covalent treated and (b) BS³ treated covalent slides.

ELISA microarray with four antibody assays (Table 1) that were previously shown to have good assay sensitivity and specificity, as well as low cross-reactivity, in multiplexed ELISA microarray [3]. The performance of the surfaces was evaluated based on spot morphology, signal to noise ratio, limit of detection, and standard curve dynamic range. Signal

intensities were evaluated by comparing single concentration assays on peptoid microsphere coated blocks with poly-L-lysine surfaces. Single point antigen concentrations correspond to the third dilution of the three-fold standard curve dilution series (i.e., approximately 11% of the maximal concentration), which has previously been shown to provide a

Table 1

Summary of the results detailing the maximal concentration of antigens, lower and upper bound, dynamic range concentrations, and single point signal intensities (11% of the maximal concentration) for the ‘uncoated’ poly-L-lysine surfaces and peptoid-based microsphere coated surfaces antigens for all 4 different assays: CD14 (cluster of differentiation 14), GFP (green fluorescent protein), HGF (hepatocyte growth factor), and RANTES (regulated on activation normal T cell expressed and secreted).

| Assay | Max Conc. (pg/mL) | Limit of Detection (pg/mL) | | Dynamic Range (pg/mL) | | Signal/Noise Ratio | |
|--------|-------------------|----------------------------|--------|-----------------------|--------|--------------------|--------|
| | | Uncoated | Coated | Uncoated | Coated | Uncoated | Coated |
| CD14 | 2500 | 1.9 | 2.0 | 527.8 | 530.2 | 21.4 | 21.3 |
| GFP | 500 | 0.2 | 0.7 | 80.0 | 97.0 | 17.8 | 30.5 |
| HGF | 1000 | 0.3 | 2.7 | 135.3 | 492.8 | 20.7 | 30.6 |
| RANTES | 500 | 0.4 | 0.3 | 64.6 | 264.2 | 15.8 | 16.8 |

strong signal intensity near saturation and in the upper usable range of the standard curve [3].

Spot morphology is dependent on the characteristics of the surface, and as such the increased topographical complexity of peptoid microsphere coated surfaces presents challenges. Although the spot morphology on peptoid microspheres is not as crisp as those on the two-dimensional poly-L-lysine surfaces (Fig. 3A), they are greatly improved over other three-dimensional surfaces [20]. The shape of the spots is still detected and analyzed by the GenePix software without any issues.

As expected, peptoid microsphere coated surfaces consistently displayed stronger signal intensities as compared to poly-L-lysine slides (Fig. 3C and Table 1). This observation is consistent for all assays independent of whether the comparisons are based on a single concentration point (Fig. 3C) or over the full standard curve (Fig. 4). However, as is the case with other three-dimensional slide surfaces, the peptoid microsphere coated surface exhibits higher background fluorescence as compared to the poly-L-lysine surface (Fig. 3B). Despite the increased background signal, the signal-to-noise ratio for the peptoid microsphere coating is the same as or higher than the poly-L-lysine coating (Table 1). More specifically, the signal-to-noise ratio is higher on the peptoid microsphere coated slides for three of the four assays tested. These data support the hypothesis that the use of peptoid microsphere coatings to increase surface area leads to improved ELISA microarray properties.

The limit of detection is defined as the lowest concentration that can be reliably detected and is a direct assessment of assay sensitivity. Evaluation of surface performance is based on previously published methods, where relative limit of detection below 2 is 'superior', between 2 and 4 is 'normal', and above 4 is 'poor' [20]. Despite the larger standard deviation observed at low antigen concentration for the peptoid microsphere coatings, they are rated in the superior category with a score of 0.9 ± 0.5 as compared to a score of 0.8 ± 0.3 for poly-L-lysine slides in our study. These values are comparable to published values for commercially available slides including poly-L-lysine (0.7 ± 0.1), aminosilane (1.3 ± 0.6), aldehyde silane (1.1 ± 0.4), epoxysilane (1.2 ± 0.6), Slide E (0.8 ± 0.4), and Full Moon (1 ± 0.7) [16].

ProMAT interprets the useful range of the standard curves as that between the lower limit of detection and upper concentration bound. As the standard curve for HGF in Fig. 4 demonstrates, and Table 1 details for all assays, the dynamic range observed for the peptoid microsphere coated surfaces is increased as compared to poly-L-lysine surfaces (2.4 pg/ml for CD14, 17 pg/ml for GFP, 357.5 pg/ml for HGF, and 199.6 pg/ml for RANTES).

4. Conclusion

Disease detection requires high-throughput assessment of multiple proteins within small sample volumes. The use of ELISA microarray and biosensors for disease detection will require the development of optimized support surfaces that allow for more generally applicable and direct immobilization procedures. While high binding affinities are imperative to prevent antibody loss and ensure robust attachment, the challenge lies in designing a microarray support that accommodates proteins of varying characteristics and provides an environment that preserves the active form of the protein. The use of peptoid microsphere coatings as a novel surface for the improvement of sandwich ELISA microarray has been evaluated. This peptoid-based, three-dimensional coating offers a customizable, robust, biocompatible interface that increases the surface area available for binding. The efficacy of the coating was assessed in terms of its overall ELISA microarray performance as compared to commercially available poly-L-lysine surfaces. The peptoid microsphere coated surfaces allowed for strong covalent antibody attachment and performed well in terms of spot morphology, signal to noise ratio, limit of detection, and standard curve dynamic range. The increase in surface area enables higher protein binding capacities as compared to poly-L-lysine surfaces, and although the peptoid microsphere coatings displayed higher background fluorescence and

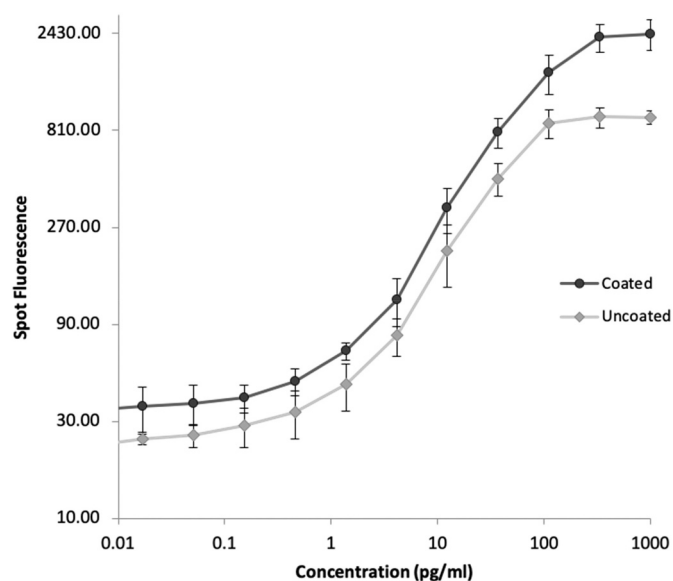


Fig. 4. Standard curves for HGF on uncoated poly-L-lysine slides and peptoid microsphere coated surfaces. Results are representative of the trends observed across all antibody assays (see Fig. S3 in Supplemental Information). Data points and cross-bars represent the means and standard deviations, respectively. The standard curves encompass data from all three replicate experiments performed using slides that were coated, printed, and processed on independent occasions.

coefficients of variation the signal-to-noise ratios were higher as compared to poly-L-lysine surfaces. Furthermore, the limits of detection were comparable to the poly-L-lysine surfaces and an improvement in dynamic range was observed for all assays tested.

The peptoid microsphere coatings provide an exciting new interface for a wide range of biosensor applications. Results suggest that commonly used biosensor protocols and procedures can be readily applied to peptoid microsphere coatings, and that the coatings outperform state-of-the-art surfaces such as poly-L-lysine. The robust peptoid microsphere coated surface provides a versatile platform that can be easily customizable to allow for various surface chemistries and incorporate different attachment sites. It offers the benefits that come with an increased surface area for binding, while at the same time allow for use of familiar chemistries that are established for both protein microarray and biosensor applications.

Supplementary data to this article can be found online at <https://doi.org/10.1016/j.sbsr.2021.100424>.

Funding

Support has been provided in part by the Arkansas Biosciences Institute, the major research component of the Arkansas Tobacco Settlement Proceeds Act of 2000. We acknowledge partial support from the Center for Advanced Surface Engineering, under the National Science Foundation Grant No. IIA-1457888 and the Arkansas EPSCoR Program, ASSET III.

Declaration of Competing Interest

The authors declare that they have no known competing financial interests or personal relationships that could have appeared to influence the work reported in this paper.

Acknowledgments

The authors would like to thank Dr. Rohana Liyanage and the Arkansas Statewide Mass Spectrometry Facility for use of and

consultation regarding MALDI, Dr. Mourad Benamara and the University of Arkansas Electron Optics Facility for use of and consultation regarding SEM, and Dr. Suresh Kumar for use of and consultation regarding CD.

References

- [1] M.F. Ullah, M. Aatif, The footprints of cancer development: cancer biomarkers, *Cancer Treat. Rev.* 35 (3) (2009) 193–200.
- [2] R. Etzioni, N. Urban, S. Ramsey, M. McIntosh, S. Schwartz, B. Reid, J. Radich, G. Anderson, L. Hartwell, Early detection: the case for early detection, *Nat. Rev. Cancer* 3 (4) (2003) 243–252.
- [3] N.B. Kiviat, C.W. Critchlow, Novel approaches to identification of biomarkers for detection of early stage cancer, *Dis. Markers* 18 (2) (2002) 73–81.
- [4] M.A. Tainsky, Genomic and proteomic biomarkers for cancer: a multitude of opportunities, *Biochim. Biophys. Acta* 1796 (2) (2009) 176–193.
- [5] A.J. Rai, D.W. Chan, Cancer proteomics: new developments in clinical chemistry, *Lab. Med.* 25 (9–10) (2001) 399–403.
- [6] J. DeRisi, L. Penland, P.O. Brown, M.L. Bittner, P.S. Meltzer, M. Ray, Y. Chen, Y. A. Su, J.M. Trent, Use of a cDNA microarray to analyze gene expression patterns in human cancer, *Nat. Genet.* 14 (4) (1996) 457–460.
- [7] M. Esteller, P.G. Corn, S.B. Baylin, J.G. Herman, A gene hypermethylation profile of human cancer, *Cancer Res.* 61 (8) (2001) 3225–3229.
- [8] B. Houser, Bio-Rad's Bio-Plex® suspension array system, xMAP technology overview, *J. Metabol. Dis.* 118 (4) (2012) 192–196.
- [9] J. Smith, D. Onley, C. Garey, S. Crowther, N. Cahir, A. Johanson, S. Painter, G. Harradence, R. Davis, P. Swarbrick, Determination of ANA specificity using the UltraPlex™ platform, *Ann. N. Y. Acad. Sci.* 1050 (1) (2006).
- [10] A. Spiro, M. Lowe, D. Brown, A bead-based method for multiplexed identification and quantitation of DNA sequences using flow cytometry, *Appl. Environ. Microbiol.* 66 (10) (2000) 4258–4265.
- [11] M.F. Elshal, J.P. McCoy Jr., Multiplex bead array assays: performance evaluation and comparison of sensitivity to ELISA, *Methods* 38 (4) (2006) 317–323.
- [12] C.A. Borrebaeck, C. Wingren, Design of high-density antibody microarrays for disease proteomics: key technological issues, *J. Proteome* 72 (6) (2009) 928–935.
- [13] B.B. Haab, Applications of antibody array platforms, *Curr. Opin. Biotechnol.* 17 (4) (2006) 415–421.
- [14] C.A. Borrebaeck, C. Wingren, High-throughput proteomics using antibody microarrays: an update, *Expert. Rev. Mol. Diagn.* 7 (5) (2007) 673–686.
- [15] S.F. Kingsmore, Multiplexed protein measurement: technologies and applications of protein and antibody arrays, *Nat. Rev. Drug Discov.* 5 (4) (2006) 310–321.
- [16] P. Pavlickova, E. Schneider, H. Hug, Advances in recombinant antibody microarrays, *Clin. Chim. Acta* 343 (1–2) (2004) 17–35.
- [17] J. Ingvarsson, A. Larsson, A.G. Sjöholm, L. Truedsson, B. Jansson, C.A. K. Borrebaeck, C. Wingren, Design of recombinant antibody microarrays for serum protein profiling: targeting of complement proteins, *J. Proteome Res.* 6 (9) (2007) 3527–3536.
- [18] W. Kusnezow, V. Banzon, C. Schröder, R. Schaal, J.D. Hoheisel, S. Rüffer, P. Luft, A. Duschl, Y.V. Sygailo, Antibody microarray-based profiling of complex specimens: systematic evaluation of labeling strategies, *Proteomics* 7 (11) (2007) 1786–1799.
- [19] C. Wingren, J. Ingvarsson, L. Dextrin, D. Szul, C.A.K. Borrebaeck, Design of recombinant antibody microarrays for complex proteome analysis: choice of sample labeling-tag and solid support, *Proteomics* 7 (17) (2007) 3055–3065.
- [20] P. Angenendt, Progress in protein and antibody microarray technology, *Drug Discov. Today* 10 (7) (2005) 503–511.
- [21] M. Sanchez-Carbayo, Antibody arrays: technical considerations and clinical applications in cancer, *Clin. Chem.* 52 (9) (2006) 1651–1659.
- [22] N.L. Anderson, The human plasma proteome: history, character, and diagnostic prospects, *Mol. Cell. Proteomics* 1 (11) (2002) 845–867.
- [23] B.B. Haab, M.J. Dunham, P.O. Brown, Protein microarrays for highly parallel detection and quantitation of specific proteins and antibodies in complex solutions, *Genome Biol.* 2 (2) (2001).
- [24] R.C. Zangar, D.S. Daly, A.M. White, ELISA microarray technology as a high-throughput system for cancer biomarker validation, *Expert Rev. Proteomics* 3 (1) (2006) 37–44.
- [25] P. Angenendt, J. Glöckler, D. Murphy, H. Lehrach, D.J. Cahill, Toward optimized antibody microarrays: a comparison of current microarray support materials, *Anal. Biochem.* 309 (2) (2002) 253–260.
- [26] Q. Xu, S. Miyamoto, K.S. Lam, A novel approach to chemical microarray using ketone-modified macromolecular scaffolds: application in micro cell-adhesion assay, *Mol. Divers.* 8 (2004) 301–310.
- [27] M. Lee, I. Shin, Fabrication of chemical microarrays by efficient immobilization of hydrazide-linked substances on epoxide-coated glass surfaces, *Angew. Chem.* 44 (2005) 2881–2884.
- [28] W. Kusnezow, J.D. Hoheisel, Solid supports for microarray immunoassays, *J. Mol. Recognit.* 16 (4) (2003) 165–176.
- [29] P. Peluso, D.S. Wilson, D. Do, H. Tran, M. Venkatasubbaiah, D. Quincy, B. Heidecker, K. Poindexter, N. Tolani, M. Phelan, K. Witte, L.S. Jung, P. Wagner, S. Nock, Optimizing antibody immobilization strategies for the construction of protein microarrays, *Anal. Biochem.* 312 (2) (2003) 113–124.
- [30] J.E. Bradner, O.M. Mcpherson, A.N. Koehler, A method for the covalent capture and screening of diverse small molecules in a microarray format, *Nat. Protoc.* 1 (5) (2006) 2344–2352.
- [31] J.E. Bradner, O.M. Mcpherson, R. Mazitschek, D. Barnes-Seeman, J.P. Shen, J. Dhaliwal, K.E. Stevenson, J.L. Duffner, S.B. Park, D.S. Neuberger, P. Nghiem, S. L. Schreiber, A.N. Koehler, A robust small-molecule microarray platform for screening cell lysates, *Chem. Biol.* 13 (5) (2006) 493–504.
- [32] S.L. Servoss, A.M. White, C.L. Baird, K.D. Rodland, R.C. Zangar, Evaluation of surface chemistries for antibody microarrays, *Anal. Biochem.* 371 (2007) 105–115.
- [33] D.J. Hill, M.J. Mio, R.B. Prince, T.S. Hughes, J.S. Moore, A field guide to foldamers, *Chem. Rev.* 101 (12) (2001) 3893–4012.
- [34] M.L. Hebert, D.S. Shah, P. Blake, J.P. Turner, S.L. Servoss, Tunable peptoid microspheres: effects of side chain chemistry and sequence, *Org. Biomol. Chem.* 11 (27) (2013) 4459.
- [35] J.A. Patch, K. Kirshenbaum, S.L. Seuryneck, R.N. Zuckermann, A.E. Barron, Versatile Oligo(N-Substituted) glycines: the many roles of peptoids in drug discovery, Nielsen: Pseudo-Peptides O-BK Pseudo-Peptides Drug Develop. (2005) 1–31.
- [36] M. Hebert, D. Shah, P. Blake, S. Servoss, Uniform and robust peptoid microsphere coatings, *Coatings* 3 (2) (2013) 98–107.
- [37] S.L. Seuryneck-Servoss, C.L. Baird, K.D. Miller, N.B. Pefaur, R.M. Gonzalez, D. O. Apiyo, H.E. Engelmann, S. Srivastava, J. Kagan, K.D. Rodland, R.C. Zangar, Immobilization strategies for single-chain antibody microarrays, *Proteomics* 8 (2008) 2199–2210.
- [38] A.M. White, D.S. Daly, S.M. Varnum, K.K. Anderson, N. Bollinger, R.C. Zangar, Promat: protein microarray analysis tool, *Bioinformatics* 22 (2006) 1278–1279.
- [39] P. Armand, K. Kirshenbaum, R.A. Goldsmith, S. Farr-Jones, A.E. Barron, K.T. V. Truong, K.A. Dill, D.F. Mierke, F.E. Cohen, R.N. Zuckermann, E.K. Bradley, NMR determination of the major solution conformation of a peptoid pentamer with chiral side chains, *Proceed. Nat. Acad. Sci.* 95 (8) (1998) 4309–4314.
- [40] C.W. Wu, T.J. Sanborn, R.N. Zuckermann, A.E. Barron, Peptoid oligomers with α -Chiral, aromatic side chains: effects of chain length on secondary structure, *J. Am. Chem. Soc.* 123 (13) (2001) 2958–2963.
- [41] K.T. Nam, S.A. Shelby, P.H. Choi, A.B. Marciel, R. Chen, L. Tan, T.K. Chu, R. A. Mesch, B.-C. Lee, M.D. Connolly, C. Kisielowski, R.N. Zuckermann, Free-floating ultrathin two-dimensional crystals from sequence-specific peptoid polymers, *Nat. Mater.* 9 (5) (2010) 454–460.
- [42] B. Sanii, R. Kudirka, A. Cho, N. Venkateswaran, G.K. Olivier, A.M. Olson, H. Tran, R.M. Harada, L. Tan, R.N. Zuckermann, Shaken, not stirred: collapsing a peptoid monolayer to produce free-floating, stable nanosheets, *J. Am. Chem. Soc.* 133 (51) (2011) 20,808–20,815.
- [43] M.L. Waters, Aromatic interactions in model systems, *Curr. Opin. Chem. Biol.* 6 (6) (2002) 736–741.
- [44] A.S. Shetty, J. Zhang, J.S. Moore, Aromatic π -stacking in solution as revealed through the aggregation of phenylacetylene macrocycles, *J. Am. Chem. Soc.* 118 (5) (1996) 1019–1027.
- [45] S. Selvarajah, O.H. Negm, M.R. Hamed, C. Tubby, I. Todd, P.J. Tighe, T. Harrison, L.C. Fairclough, Development and validation of protein microarray technology for simultaneous inflammatory mediator detection in Human Sera, *Mediat. Inflamm.* 2014 (2014) 1–12.
- [46] G.G. Claessens, J.F. Stoddart, π - π interactions in self-assembly, *J. Phys. Org. Chem.* 10 (5) (1997) 254–272.
- [47] G.R. Perez Bakovic, J.L. Roberts, B. Colford, M. Joyce, S.L. Servoss, Peptoid microsphere coatings: the effects of helicity, temperature, pH, and ionic strength, *Biopolymers* 110 (6) (2019).